PAGEOPH, Vol. 127, Nos. 2/3 (1988)

0033-4553/88/030219-36$1.50 + 0.20/0

Global Model of the Thermosphere-Ionosphere-Protonosphere System

A. A. NAMGALADZE[1], YU. N. KORENKOV[1], V. V. KLIMENKO[1], I. V. KARPOV,[1] F. S. BESSARAB,[1] V. A. SUROTKIN,[1] T. A. GLUSHCHENKO,[1] and N. M. NAUMOVA[1]

Abstract—In this paper the formulation of the problem and preliminary numerical computation results of the thermosphere-ionosphere-protonosphere system parameters are discussed.

The model constructed describes time-dependent distributions of the multicomponent near-earth space plasma parameters by means of numerical integration of the appropriate three-dimensional plasma hydrodynamic equations. In the thermospheric block of the model, global distribution of neutral gas temperature and N_2, O_2, O concentrations, as well as three-dimensional circulation of the neutral gas are calculated in the range of height from 80 km to 520 km. In the ionospheric section of the model, global time-dependent distribution of ion and electron temperatures, as well as molecular and atomic O^+, H^+ ion concentrations are calculated. Global two-dimensional distribution of electric potential is calculated taking into account computed thermosphere and ionosphere parameters.

The inputs needed for our global model are the solar EUV spectrum; the auroral precipitation pattern; the distribution of the field-aligned currents and the model of the geomagnetic field.

Preliminary results are obtained without regard to electromagnetic plasma drift for the solar minimum, low geomagnetic activity and spring equinox conditions. Global distributions of the calculated parameters in the magnetic dipole latitude-longitude frame are presented for 1200 UT. In the summary ignored processes and future direction are discussed.

Key words: Model, thermosphere, ionosphere, protonosphere.

1. Introduction

Over the last years the emphasis in modelling of the near-earth space has shifted to the problems of the global models construction, due to intensive development of the computer means and numerical methods of solution of multidimensional equations. A number of large-scale mathematical models of the thermosphere and ionosphere has been constructed of late, but nonselfconsistent. Several global three-dimensional models describing neutral temperature, composition and wind in the thermosphere have been developed (SEREBRYAKOV, 1982; KOLESNIK and KOROLEV, 1983; FULLER-ROWELL and REES, 1980; 1983; DICKINSON *et al.*, 1981; 1984; KARPOV

[1] Kaliningrad Observatory of Institute of Terrestrial Magnetism, Ionosphere and Radio Wave Propagation, Academy of Science USSR, (KMIO IZMIR AN USSR), pr. Pobedy, 41, Kaliningrad, 236017 USSR.

et al., 1987). These models were meant to describe the thermosphere parameters variations at the heights of the ionospheric *F*-region due to used approaches. The modelling of the magnetized plasma distribution in the ionosphere has taken the line of the development of the regional model construction, such as models of equatorial ionosphere (ANDERSON, 1973; 1981; SUROTKIN *et al.*, 1979); models of midlatitude *F*-region ionosphere (STUBBE, 1970; SCHUNK and WALKER, 1973; NAMGALADZE *et al.*, 1977); models of the ionosphere-plasmasphere mid-latitude system as a whole (MOFFETT and MURPHY, 1973; POLJAKOV *et al.*, 1975; BAILEY, 1978; KRINBERG and TASCHCHILIN, 1980; YOUNG *et al.*, 1980; QUEGAN *et al.*, 1982; and others); models of the high-latitude *F*2-region ionosphere (KNUDSEN, 1974; KNUDSEN *et al.*, 1977; MOZHAEV and OSIPOV, 1977; SOJKA *et al.*, 1981a, b, c; KOLESNIC and GOLIKOV, 1982; SCHUNK and RAITT, 1980) and models of the high-latitude ionosphere-protonosphere system (MARUBASHI, 1979; KLIMENKO and NAMGALADZE, 1980; NAMGALADZE *et al.*, 1980; KLIMENKO, 1983). The first steps toward the global ionospheric model creation have been made by SAENKO *et al.* (1980) and SOJKA and SCHUNK (1985).

The general property of all mentioned ionospheric models has been an application of the neutral atmospheric parameters from semi-empirical models of the thermosphere (JACCHIA, 1977; HEDIN *et al.*, 1977 and others) and parameters of the electric field of the magnetospheric convection from the models by VOLLAND (1975; 1978) and equatorial electric field from models of FEJER *et al.* (1979), RICHMOND *et al.* (1980), and WAGNER *et al.* (1980). At the same time there are many theoretical models of the permanent magnetosphere convection electric field (Wolf, 1970; WOLF and JAGGI, 1973; LAYTSKY, 1978; GIZLER *et al.*, 1979; MOZHAEV and OSIPOV, 1981), nonstationary magnetospheric convection field models such as by HAREL *et al.* (1981), PUDOVKIN and ZAKHAROV (1984), as well as electric dynamo field models by TAKEDA (1982), GLUSHAKOV (1979), and RICHMOND *et al.* (1976).

The modern task requires the coupling of large-scale flow ionospheric models of the separate regions, thermospheric models and model of the global electric field in the united model of the solar-terrestrial system. Basic approaches of constructing this model have been formulated in the paper by NAMGALADZE *et al.* (1985). In this paper we describe what appears to be the numerical model of the Thermosphere-Ionosphere-Protonosphere system.

In our model, the thermal charged and neutral components of the upper atmosphere are considered self-consistently from high to low latitudes on a global scale at altitudes between 80 kilometers and 15 R_E (where R_E is the radius of the Earth), without the action of the electric field in the first stage and also taking into account self-consistence calculation of the global electric field potential in the second stage. This model is constructed to study the large-scale disturbances of the thermosphere-ionosphere-protonosphere system which are connected with solar flares, magnetic storms and substorms.

The model equations, coordinate systems, initial and boundary conditions, methods of the solution model equations, and basic algorithm are described in

Section 2. In Section 3 we present preliminary results of our model calculations for spring equinox, solar minimum and low geomagnetic activity without plasma convection. In Section 4 we discuss our results. Conclusion and our future directions are presented in Section 5.

2. *The Model Description*

2.1 Theoretical Formulation

In the thermospheric block of the model, the space-time-dependent O_2, N_2, O neutral densities, T_n-neutral temperature and $\vec{V}_n$-thermospheric circulation vector are computed by solving the appropriate continuity, momentum and energy equations over the altitude range of 80 to 520 km. For densities of neutral hydrogen we have adopted the barometric law from the semi-empirical model J77 (JACCHIA, 1977).

The ionospheric block of the model calculates space-time-dependent O^+, H^+, XY^+ (summary molecular) ion densities, T_i, T_e—ion and electron temperatures, $\vec{V}_i$—vector of the ion velocity by solving the corresponding hydrodynamical equations along flux tubes from 175 km in one hemisphere to 175 km in the conjugate hemisphere. The electron density is obtained from the requirement of charge neutrality. The theoretical electric potentials are computed by solving Puasson's equation.

A number of parameters are required as inputs to this model. They are EUV solar radiation, resonantly scattered radiation, auroral precipitation and field-aligned current density at the top of the ionospheric conducting auroral region. The basic equations for the neutral and charged species, as well as for the electrical potential are reproduced in the vector formulation.

Continuity equations

$$\frac{\partial n_n}{\partial t} + \nabla(n_n(\vec{V} + \vec{V}_n)) = Q_n - L_n \tag{1}$$

$$\frac{\partial N_i}{\partial t} + \nabla(N_i\vec{V}_i) = Q_i - L_i \tag{2}$$

where the subscripts n and i label the neutral and charged constituents, respectively. The $\vec{V}$, n_n, $\vec{V}_n$, N_i, $\vec{V}_i$, $Q_{n,i}$, $L_{n,i}$ are mean mass velocity of the neutral gas, the concentration and diffusion velocity of the n-th species, the flux velocity of the i-th ion species, production and loss rates, respectively.

Momentum equations

$$\rho\left[\frac{\partial\vec{V}}{\partial t} + (\vec{V},\nabla)\vec{V} + 2\vec{\Omega}\times\vec{V}\right] = \rho\vec{g} - \nabla P - \sum_n\sum_i \mu_{ni}n_n\nu_{ni}(\vec{V} - \vec{V}_i) + \eta\nabla^2\vec{V} \tag{3}$$

$$N_i M_i \frac{\partial \vec{V}_i}{\partial t} = N_i M_i (\vec{g} - 2\vec{\Omega} \times \vec{V}_i - \vec{\Omega} \times \vec{\Omega} \times \vec{r}) - \nabla P_i -$$

$$- \sum_k \mu_{ik} N_i \nu_{ik} (\vec{V}_i - \vec{V}_k) - \sum_n \mu_{in} N_i \nu_{in} (\vec{V}_i - \vec{V}) + eN_i (\vec{E} + \vec{V}_i \times \vec{B}) \quad (4)$$

$$- \nabla P_e - eN_e (\vec{E} + \vec{V}_e \times \vec{B}) = 0 \quad (5)$$

where

$$P = kT_n \sum_n n_n; \qquad \rho = \sum_n n_n m_n;$$
$$P_i = N_i k T_i; \qquad P_e = k T_e N_e.$$

There are

m_n, M_i —masses of the neutral and charged particles species n and i, respectively;
μ_{nl} —reduced mass;
$\vec{\Omega}$ —The earth's angular velocity vector;
$\vec{r}$ —a radius vector from the center of the earth to the point where the equations are applied;
$\vec{g}$ —the acceleration due to gravity;
k —Boltzmann's constant;
ν_{nl}, ν_{ni} —collision frequencies;
η —the coefficient of viscosity;
T_n, T_i, T_e —temperatures of neutral particles, ion and electrons, respectively;
P, P_i, P_e —mean mass pressure of the neutral gas, pressure of ion and electron gases, respectively;
ρ —mass density of the neutral gas;
e —electron charge;
$\vec{E}$, $\vec{B}$ —electric and magnetic fields.

Energy equations

For neutral gas:

$$\rho c_v \left(\frac{\partial T_n}{\partial t} + (\vec{V}, \nabla) T_n \right) + P \nabla \vec{V} = \nabla (\lambda_n \nabla T_n) + P_{nQ}^{\mathrm{UV}} + P_{nQ}^{J} + P_{nQ}^{c} + P_{nL}. \quad (6)$$

For ion gas:

$$\frac{3}{2} N_i k \frac{dT_i}{dt} + N_i k T_i \nabla \vec{V}_i = \nabla (\lambda_i \nabla T_i) + P_{iQ}^{J} + P_{iT}^{e} + P_{iT}^{n} + P_{iT}^{k}. \quad (7)$$

For electron gas:

$$\frac{3}{2}N_e k\frac{dT_e}{dt} + N_e k T_e \nabla V_e = \nabla(\lambda_e \nabla T_e) + P^s_{eQ} + P^i_{eT} + P^n_{eT} \tag{8}$$

where

c_v —is the specific heat at constant volume;
$\lambda_n, \lambda_i, \lambda_e$ —thermal conductivity of neutral, ion and electron gases, respectively;
P^{UV}_{nQ} —the rate of heating of neutral gas by EUV solar radiation;
P^c_{nQ} —the rate of heating of neutral gas by precipitation auroral electrons;
P^J_{nQ}, P^J_{iQ} —Joule heating;
P_{nL} —the rate of heat loss of neutral gas due to radiation;
$P^n_{iT}, P^e_{iT}, P^i_{eT}, P^k_{eT}$ —the rates of the heat exchange between different gases;
P^s_{eQ} —the rate of heating electron gas by suprathemal electron

$$P^i_{eT} = -P^e_{iT}; \qquad P^k_{iT} = -P^i_{kT}.$$

Electric potential and current density equations. In the quasi-stationary state the continuity equation of the current is

$$\nabla\vec{J} = 0 \tag{9}$$

and

$$\vec{J} = \vec{J}_i + \vec{J}_m \tag{10}$$

where

$$\vec{J}_i = \hat{\sigma}_i(\vec{E} + \vec{V} \times \vec{B})$$

$\vec{J}_i$ —ionospheric current density;
$\vec{J}_m$ —magnetospheric current density;
$\hat{\sigma}_i$ —ionospheric conduction tensor.

The mathematical problem reduces to the condition that the electric field $\vec{E}$ can be derived from an electric potential φ, that is

$$\vec{E} = -\nabla\varphi. \tag{11}$$

Then (9) becomes

$$\nabla[\hat{\sigma}_i(\nabla\varphi - \vec{V} \times \vec{B}) - \vec{J}_m] = 0. \tag{12}$$

In all mentioned equations $\vec{B}$ is the geomagnetic central dipole field and given by the equation

$$\vec{B} = -M(2\cos\theta\vec{e}_r + \sin\theta\vec{e}_\theta)/r^3 \tag{13}$$

where M—is dipole moment and $\vec{e}_r, \vec{e}_\theta, \vec{e}_\lambda$—orthogonal set of unit vectors of spherical geomagnetic coordinate system.

2.2 Coordinate Systems

One of the principal features of our model is that different groups of the modelling equations are solved in various coordinate systems with interpolation of the necessary parameters from one system to the other. The neutral continuity momentum and energy equations, as well as molecular ion continuity, momentum and energy equations, and equation for the electric potential are solved in the *spherical geomagnetic coordinate system*, because one of the energy and momentum sources for the neutral atmosphere are auroral precipitation inputs as well as energy and momentum of the molecular ions. These sources have symmetry in the geomagnetic frame. This frame is also quite natural for the electric potential equation.

The atomic ion continuity, momentum, ion and electron temperature equations are solved in the *magnetic dipole coordinate system*, as in this case the geomagnetic field has a very strong effect on the behaviour and distribution of magnetized charge particles, besides, the input parameters to our global model are associated with two other reference frames, i.e., *geographic and solar-magnetic frames*. The solar zenith angle has symmetry relatively of a subsolar point of geographic frame, just as auroral precipitation inputs pertain to a solar-magnetic coordinate system that is fixed relative to the Sun.

The transformation of the spherical geomagnetic coordinates r, θ, λ into the magnetic dipole coordinates q, u, v are given by the following expressions

$$q = \left(\frac{R_E}{r}\right)^2 \cos\theta; \qquad u = \left(\frac{R_E}{r}\right) \sin^2\theta; \qquad v = \lambda; \tag{14}$$

where q, u, v—dimensionless magnetic potentials so that q represents the surfaces of the constant magnetic potential and the family of curves which represents the dipole magnetic lines of force is given by u = constant. There are R_E—radius of the Earth, r—distance from centre of the Earth, θ, λ—geomagnetic co-latitude and longitude, respectively. The transformation between other coordinate systems, that are used in our model, are given by standard formulas.

2.3 Model Equations in the Coordinate Systems

In the next subsections, we briefly describe model equations in the various coordinate systems.

Neutral model equations in the spherical geomagnetic coordinates. The system of the equations (1), (3), and (6) describes all ranges of dynamics phenomena in the upper atmosphere. However, these equations can be simplified because of the greatly different scale lengths in vertical and horizontal directions. Furthermore, additional simplifications can be obtained, since the magnitude of the vertical component of the neutral gas velocity is generally much smaller than the magnitude of either horizontal velocity components. Moreover, characteristic times of considered processes are so large that one may assume hydrostatic equilibrium. Considering the above simplifications, we write equations (1), (3), and (6) in the spherical geomagnetic coordinate system.

Continuity equation

$$\frac{\partial n_n}{\partial t} + \frac{\partial n_n}{\partial r}(V_r + V_n) + \frac{1}{r \sin\theta}\left[\frac{\partial (n_n V_\theta \sin\theta)}{\partial \theta} + \frac{\partial (n_n V_\lambda)}{\partial \lambda}\right] = Q_n - L_n \tag{15}$$

where

$$V_n = V_{nm} + V_{nT}$$

and

V_{nm}, V_{nT} —the n-th species molecular and eddy diffusion velocity, respectively;
Q_n, L_n —production and loss rates due to chemical reactions.

Momentum equations

$$\frac{\partial V_\theta}{\partial t} + V_r\frac{\partial V_\theta}{\partial r} + \frac{V_\theta}{r}\frac{\partial V_\theta}{\partial \theta} + \frac{V_\lambda}{r\sin\theta}\frac{\partial V_\theta}{\partial \lambda} + 2\Omega_r V_\lambda - 2\Omega_\theta V_r + \frac{V_\theta V_\lambda}{2}\operatorname{ctg}\theta = -\frac{1}{\rho r}\frac{\partial P}{\partial \theta} + \frac{1}{\rho}\frac{\partial}{\partial r}\left(\eta\frac{\partial V_\theta}{\partial r}\right) + F_{n\theta} \tag{16}$$

$$\frac{\partial V_\lambda}{\partial t} + V_r\frac{\partial V_\lambda}{\partial r} + \frac{V_\theta}{r}\frac{\partial V_\lambda}{\partial \theta} + \frac{V_\lambda}{r\sin\theta}\frac{\partial V_\lambda}{\partial \lambda} - 2\Omega_r V_\theta + 2\Omega_\theta V_r + \frac{V_\theta^2 + V_\lambda^2}{2} = -\frac{1}{\rho r\sin\theta}\frac{\partial P}{\partial \lambda} + \frac{1}{\rho}\frac{\partial}{\partial r}\left(\eta\frac{\partial V_\theta}{\partial r}\right) + F_{n\lambda} \tag{17}$$

where

$F_{n\theta}$, $F_{n\lambda}$ —components of the force of interaction with charged particles.

For the calculation of the vertical component of the mean mass velocity, the continuity equation for the mass density is used.

The energy equation

$$\rho c_v\left(\frac{\partial T}{\partial t} + V_r\frac{\partial T}{\partial r} + \frac{V_\theta}{r}\frac{\partial T}{\partial \theta} + \frac{V_\lambda}{r\sin\theta} + \frac{\partial T}{\partial \lambda}\right) + \rho\left(\frac{\partial V_r}{\partial r} + \frac{1}{r\sin\theta}\left(\frac{\partial V_\theta \sin\theta}{\partial \theta} + \frac{\partial V\lambda}{\partial \lambda}\right)\right)$$
$$= \frac{\partial}{\partial r}\left[(\lambda_n + \rho c_p K_T)\frac{\partial T}{\partial r} + \rho g K_T\right] + P_{nQ}^{UV} + P_{nQ}^{J} + P_{nQ}^{c} + P_{nL} \qquad (18)$$

where

c_p —is specific heat at constant pressure;
K_T —is eddy diffusion coefficient.

Efficients for the P_{nQ}^{UV} and P_{nQ}^{c} are 0.6 by dissociation UV heating, 0.5 by ionization EUV heating and 0.6 by precipitation heating.

The loss rates radiation by O (λ = 6300 Å) and CO_2 (1500 Å) are calculated by GORDIETS *et al.* (1982).

Diffusion processes. Neglecting horizontal diffusion processes, we write vertical diffusion flux in form

$$n_n V_{nm} = -\sum_l \mathscr{D}_{nl}\left\{\frac{\partial n_l}{\partial r} + \frac{n_l}{H_l} + (1 + \alpha_{Tl})\frac{n_l}{T}\frac{\partial T}{\partial r}\right\} \qquad (19)$$

$$n_n V_{nT} = -K_T\left\{\frac{\partial n_n}{\partial r} + \frac{n_n}{H} + \frac{n_n}{T}\frac{\partial T}{\partial r} - \frac{n_n}{m}\frac{\partial m}{\partial r}\right\} \qquad (20)$$

where

$\mathscr{D}_{nl}$ —molecular diffusion coefficient;
α_{Tl} —thermodiffusion factor;
H_l —the scale height of the l-th species;
H —average scale height;
m —average molecular mass.

The coefficients $\mathscr{D}_{nl}$ for O, O_2 and N_2 species are the same as in the paper by VLASOV and DAVYDOV (1981). Thermodiffusion factors are assumed 0.12 for O_2, 0.08 for N_2 and 0.08 for atomic oxygen. The eddy diffusion coefficient is assumed in the form of SHIMAZAKI (1977).

$$K_T = K_m \exp(-S_1(z - z_m)^2), \qquad z \geqslant z_m \qquad (21)$$

$$K_T = (K_m - K_0)\exp(-S_2(z - z_m)^2) + K_0 \exp(S_3(z - z_m)), \qquad z < z_m \qquad (22)$$

where K_m, K_0, h_m, S_1, S_2, S_3 are empirical constants.

Photochemical processes in the neutral atmosphere. The simple scheme of the photochemical processes is used in our thermospheric model. There is dissociation of the O_2 by solar radiation between 1350 and 2400 Å

$$O_2 + h\nu \rightarrow O + O, \tag{R1}$$

reaction of the recombination of atomic oxygen by three-collision

$$O + O + M \xrightarrow{k_2} O_2 + M \tag{R2}$$

with $k_2 = 9.9 \cdot 10^{-34} \exp(470/T)$ cm^6 sec^{-1} (OGAWA and SHIMAZAKI, 1975), reaction of the recombination of atomic oxygen and molecular oxygen by three collision

$$O + O_2 + M \xrightarrow{k_3} O_3 + M \tag{R3}$$

with rate coefficient $k_3 = 1.1 \cdot 10^{-34} \exp(510/T)$ cm^6 sec^{-1}, (OGAWA and SHIMAZAKI 1975), and reaction of the radiative recombination of the atomic oxygen

$$O + O \xrightarrow{k_4} O_2 + h\nu \tag{R4}$$

with rate coefficient $k_4 = 10^{-20}$ cm^3 sec^{-1} (IVELSKAYA *et al.*, 1970).

Continuity equations for molecular ions. The continuity equation for the molecular ions without the divergence of plasma flux can be written

$$\frac{\partial [XY^+]}{\partial t} = Q_s + Q_f - L \tag{23}$$

where

$$\begin{aligned} [XY^+] &= [NO^+] + [O_2^+] + [N_2^+] \\ Q_s &= q(NO^+) + q(O_2^+) + q(N_2^+) \\ Q_f &= (k_5[N_2] + k_6[O_2])[O^+] \\ L &= \alpha_{ef}[XY^+][N_e]. \end{aligned}$$

In these expressions $[XY^+]$ is the summary concentration of molecular ions, Q_s is total ions production rate by solar EUV radiation and auroral precipitations, Q_f is photochemical production rate, L is recombination loss rate and α_{ef} is effective recombination coefficient.

Model equations in the dipole coordinate system. Continuity equations for the atomic ionospheric ions can be written in the form

$$\frac{\partial N_i}{\partial t} + \vec{V}_\perp \nabla N_i = Q_i - L_i - B\frac{\partial}{\partial s}\left(\frac{N_i V_i^{\parallel}}{B}\right) - N_i \nabla \vec{V}_\perp \tag{24}$$

where

$\vec{V}_\perp$ —is electromagnetic drift velocity;

$V_i^{\parallel}$ —is the component of the ion motion velocity along $\vec{B}$;
s —is the distance along magnetic flux tube.

The operator $\partial/\partial t + \vec{V}_\perp \nabla$ is replaced by D/Dt in Lagrange reference system, connected with the geomagnetic field and moving with the velocity $\vec{V}_\perp$. Now D/Dt means the time derivative along the drift trajectory, that is convective derivative. As a result, we have the continuity equation of the next form

$$\frac{DN_i}{Dt} = Q_i - L_i - B\frac{\partial}{\partial s}\left(\frac{N_i V_i^{\parallel}}{B}\right) - N_i \nabla \vec{V}_\perp. \tag{25}$$

Equations of motion. Projecting the equation of motion (4) on geomagnetic field line term by term, we obtain in the described above Lagrange frame of reference

$$M_i N_i\left(\frac{DV_i^{\parallel}}{Dt} + V_i^{\parallel}\frac{\partial V_i^{\parallel}}{\partial s}\right) = M_i N_i g^* \sin I - \frac{\partial P_i}{\partial s} - \frac{N_i}{N_e}\frac{\partial P_e}{\partial s} - M_i N_i (2V_u \Omega_\lambda + 2V_v \Omega_r \cos I - \Omega_r \Omega_\theta r \cos I) - M_i(Q_i - L_i)V_i^{\parallel} - M_i N_i V_i^{\parallel}\frac{1}{2}\nabla \vec{V}_\perp - \sum_{j \neq i}\mu_{ij} v_{ij} N_i (V_i^{\parallel} - V_j^{\parallel}) - \sum_n \mu_{in} v_{in} N_i (V_i^{\parallel} - V_n^{\parallel}) \tag{26}$$

where

$$g^* = g - \frac{3}{r}[(1 + \cos^2\theta)/(1 + 3\cos^2\theta)V_u^2 + V_v^2/2] + 2V_v\Omega_\theta - (\Omega^2 - \Omega_r^2)\cdot r$$

I —is the angle of inclination;
V_v, V_u —are components of the electromagnetic drift velocity in the magnetic dipole coordinate system;
Ω_r, Ω_θ,Ω_λ —components of the earth's angular velocity vector in the spherical geomagnetic coordinate system;
$V_i^{\parallel}$, $V_j^{\parallel}$, $V_n^{\parallel}$ —components of the motion velocity vectors of the i-th and j-th ion species and the n-th neutral species along the geomagnetic field, respectively.

Thermal balance equations for ion gas. Assuming temperatures of different atomic ion species equal, and using thermal balance equations (7), we obtain a single equation for atomic ion temperature in the above-mentioned Lagrange frame of reference

$$\frac{3}{2}k\sum_j N_j\left(\frac{DT_i}{Dt} + \frac{\sum_j (N_j V_j^{\parallel})}{\sum_j N_j}\frac{\partial T_i}{\partial s}\right) + T_i \sum_j N_j k\left(B\frac{\partial}{\partial s}\left(\frac{V_j^{\parallel}}{B}\right) + \nabla \vec{V}_\perp\right) = B\frac{\partial}{\partial s}\left(\sum_j \lambda_j \frac{1}{B}\frac{\partial T_i}{\partial s}\right) + \sum_j (P_{jT}^n + P_{jT}^e + P_{jQ}^J) \tag{27}$$

where

$$P^n_{iT} = N_i \sum_n \nu_{in}\mu_{in}/(m_i + m_n)\cdot 3k(T_n - T_i);$$

$$P^e_{iT} = N_i \frac{m_e}{M_i}\nu_{ie}\, 3k\,(T_e - T_i);$$

$$P^J_{iQ} = N_i\left(\sum_n \frac{\mu_{in}m_n}{M_i + m_n}\nu_{in}(\vec{V}_n - \vec{V}_i)^2 + \sum_j \frac{\mu_{ij}M_j}{M_i + M_j}\nu_{ij}(\vec{V}_j - \vec{V}_i)^2\right)$$

where ν_{in}, ν_{ie} are calculated from the expression given by STUBBE (1970).

Electron thermal balance equation. We write equation (8) in the dipole coordinates, taking into account that

$$V^{\parallel}_e = \sum_j N_j V^{\parallel}_j / N_e$$

and passing to the Lagrange frame of reference

$$\frac{DT_e}{Dt} + \frac{\sum_i N_i V^{\parallel}_i}{N_e}\frac{\partial T_e}{\partial s} + \frac{2}{3}\left(\nabla\vec{V}_{\perp} + B\frac{\partial}{\partial s}\left(\frac{\sum_j N_i V^{\parallel}_i}{BN_e}\right)\right)T_e$$
$$= \frac{B}{N_e}\frac{\partial}{\partial s}\left(\frac{\lambda_e}{3/2kB}\frac{\partial T_e}{\partial s}\right) + \frac{2}{3kN_e}(P^i_{eT} + P^n_{eT} + P^s_{eQ}) \quad (28)$$

where $P^i_{eT} = -P^e_{iT}$, $P^n_{eT} = -P^e_{nT}$ are the rates of the energy loss due to rotational, vibrational excitation of the molecules O_2 and N_2, as well as rates due to fine structure and electron state excitation of the atomic oxygen, given by STUBBE and WARNUM (1972). $P^s_{eQ} = P^s_{\text{loc}} + P^s_{n\text{loc}}$ is the summary rate of the heating of electron gas by photoelectrons in the local approximation of STUBBE (1970) and nonlocal heating by escaping photoelectrons in the form given by MATAFONOV (1986).

Equations for drift trajectories. In the chosen Lagrange reference system we have

$$\frac{D}{Dt} = \frac{\partial}{\partial t} + \vec{V}_{\perp}\nabla = \frac{\partial}{\partial t} + \frac{V_v}{h_v}\frac{\partial}{\partial v} + \frac{V_u}{h_u}\frac{\partial}{\partial u} \quad (29)$$

where h_u and h_v are the Lame coefficients in the dipole coordinate system

$$h_u = r^2/(R_E \sin\theta\sqrt{1 + 3\cos^2\theta})$$
$$h_v = r\sin\theta.$$

At the same time we have

$$\frac{D}{Dt} = \frac{\partial}{\partial t} + \frac{dv}{dt}\frac{\partial}{\partial v} + \frac{du}{dt}\frac{\partial}{\partial u}. \quad (30)$$

Comparing (29) and (30) we obtain equations for the drift trajectories

$$\frac{dv}{dt} = \frac{V_v}{h_v}; \qquad \frac{du}{dt} = \frac{V_u}{h_u}. \tag{31}$$

We notice that the q-coordinate does not change along drift trajectories.

To calculate parameters of ionospheric drift plasma at a given location r, θ, λ in the near-earth space, we specify a discrete grid with dipole coordinates (u_i, q_i, v_i) in nodes. For each u_i, q_i, v_i we integrate the trajectory equations (31), retroactively to obtain initial conditions plasma parameters for the model equations (24–28).

Photochemical processes for charged particles. In our ionospheric model the following photochemical processes are used. The reactions of the atomic oxygen ions O^+ with moleculars O_2 and N_2

$$O^+ + O_2 \xrightarrow{k_5} O_2^+ + O \tag{R5}$$

$$O^+ + N_2 \xrightarrow{k_6} NO^+ + N. \tag{R6}$$

Reaction rates k_5 and k_6 can be approximated by the expressions from the paper by TORR and TORR (1979).

Reactions of the charge exchange between O^+ and H, and H^+ and O

$$O^+ + H \xrightarrow{k_7} H^+ + O \tag{R7}$$

$$H^+ + O \xrightarrow{k_8} O^+ + H. \tag{R8}$$

Reaction rates k_7 and k_8 are analogous to those from SCHUNK and WALKER (1972). The reaction of the dissociative recombination for molecular ions

$$XY^+ + e \xrightarrow{\alpha_{ef}} X + Y$$

where $\alpha_{ef} \approx \alpha(NO^+)$ by the analogy from TORR and TORR (1979).

The equation for electric potential. As was noted earlier, the equation for electric potential is solved in a spherical geomagnetic coordinate system. Assuming that the radial component of ionospheric conduction current is small in comparison with horizontal currents in the first approximation, we have for the conductivity tensor in the spheric geomagnetic coordinate system

$$\hat{\sigma}_i = \begin{pmatrix} \tilde{\sigma}_{\theta\theta} & \tilde{\sigma}_{\theta\lambda} \\ \tilde{\sigma}_{\lambda\theta} & \tilde{\sigma}_{\lambda\lambda} \end{pmatrix} \tag{32}$$

where

$$\tilde{\sigma}_{\theta\theta} = \frac{\sigma_{\|}\sigma_P}{\sigma_{\|}\sin^2 I + \sigma_P \cos^2 I}$$

$$\tilde{\sigma}_{\theta\lambda} = -\tilde{\sigma}_{\lambda\theta} = -\frac{\sigma_{\|}\sigma_H \sin I}{\sigma_{\|}\sin^2 I + \sigma_P \cos^2 I}$$

$$\tilde{\sigma}_{\lambda\lambda} = \frac{\sigma_{\|}\sigma_P \sin^2 I + (\sigma_P^2 + \sigma_H^2)\cos^2 I}{\sigma_{\|}\sin^2 I + \sigma_P \cos^2 I}.$$

Here $\sigma_{\|}$, σ_P and σ_H are conductivities along geomagnetic field, Pedersen and Hall, respectively.

Assuming that currents are absent below the current-carrying layer of the ionosphere, and integrating the equation (12) over the height of the current-carrying layer between its low boundary r_1 and the top one r_2, acknowledging that the electric field components change very weakly with the height, we write the Puassone equation (10) for the electric field potential in the spherical geomagnetic coordinate system in the form

$$\frac{\partial}{\partial\theta}\left(\alpha\frac{\partial\varphi}{\partial\theta}\right) + \gamma\frac{\partial\varphi}{\partial\theta} + \frac{\partial}{\partial\lambda}\left(\beta\frac{\partial\varphi}{\partial\lambda}\right) - \delta\frac{\partial\varphi}{\partial\lambda} = \psi - r_2^2 \sin\theta \sin I J^{\|}(r_2). \tag{33}$$

Here

$$\alpha = \sin\theta\Sigma_{\theta\theta}; \qquad \beta = \frac{\Sigma_{\lambda\lambda}}{\sin\theta};$$

$$\gamma = \frac{\partial\Sigma_{\lambda\theta}}{\partial\lambda}; \qquad \delta = \frac{\partial\Sigma_{\lambda\theta}}{\partial\theta};$$

$$\psi = r_2\frac{\partial}{\partial\theta}\left(\sin\theta\int_{r_1}^{r_2} B(-\tilde{\sigma}_{\theta\theta}V_\lambda \sin I + \tilde{\sigma}_{\theta\lambda}(V_\theta \sin I - V_r \cos I))\,dr\right)$$

$$+ r_2\frac{\partial}{\partial\lambda}\left[\int_{r_1}^{r_2} B(-\tilde{\sigma}_{\lambda\theta}V_\lambda \sin I + \tilde{\sigma}_{\lambda\lambda}(V_\theta \sin I - V_r \cos I))\,dr\right]$$

where $\Sigma_{\theta\theta}$, $\Sigma_{\lambda\theta}$ and $\Sigma_{\lambda\lambda}$ are height integrated conductivities $\tilde{\sigma}_{\theta\theta}$, $\tilde{\sigma}_{\lambda\theta}$ and $\tilde{\sigma}_{\lambda\lambda}$ respectively. $J^{\|}(r_2)$ is the field aligned current at $r = r_2$. On poles there is set electric potential which equals its mean value, borrowed from the neighbouring latitudinal circle.

2.4 Global Inputs

For the initial study of the global thermosphere-ionosphere-protonosphere system, we have chosen solar minimum, low magnetic activity and spring equinox conditions. For solar minimum we take F10.7 = 100, while for low magnetic activity we assume that $K_p = 1$.

The ionization production rates of ion species have been calculated with the

solar EUV spectrum of TORR and TORR (1979). Intensities of night sky HL_α 1216 Å, HL_β 1026 Å, HeI 584 Å, HeII 304 Å radiation were chosen 5 kR for HL_α and 5R for the others.

The auroral ion production rate profiles are calculated by the method of DEMINOV and HEGAI (1981) with the exponential spectrum. Characteristic energies of 0.2 keV and 5 keV are associated with precipitating electrons in the cusp and night auroral zone, respectively. Adopted auroral precipitating energy fluxes are typical for low geomagnetic activities and correspond to HARDY and GUSSENHOVEN (1985).

The location of the zones and the magnitudes of the currents have been chosen to obtain the distribution of electric fields close to actually observed. The first zone of field-aligned currents, flowing into the ionosphere on the dawn side and flowing out on the dusk one, is on $\pm 75°$ magnetic latitude. The second zone of the field-aligned currents, flowing into the ionosphere on the dusk side and outflowing on the dawn side, is on $\pm 65°$ magnetic latitude (IIJIMA and POTEMRA, 1976).

2.5 Initial and Boundary Conditions and Methods for the Solution of Modelling Equations

In the neutral submodel at the upper boundary we assume that

$$\frac{\partial \vec{V}}{\partial_r} = 0; \qquad \frac{\partial T_n}{\partial_r} = 0.$$

At the lower boundary empirical models of temperature and composition are used.

For the initial condition of the neutral submodel we use the MSIS empirical model of temperature and composition at and above 120 km and the model of ALCAYDE (1981) below 120 km, decked with MSIS model at height 120 km.

As mentioned above, integration of the model ionospheric equations is carried out along dipole geomagnetic field lines. We assume that field lines with L = 15 (L—parameter of McIlwain) are open. The boundary conditions on close field lines are given near the bases of the lines in the north and south hemispheres on the height of 175 km. For the equations of continuity, the atomic concentrations are obtained from photochemical equilibrium conditions. The values of ion and electron temperatures are calculated from the equations of heat balance, without providing for heat conductivity. On the open field lines the boundary conditions near the bases of lines are set as on the closed lines. On the gap ($r \approx 15\ R_E$) there are set zero ion concentrations and zero heat fluxes.

Initial conditions may be chosen arbitrarily. For example, zero ion concentrations and ion and electron temperatures equal the temperature of neutral gas.

The system of the modelling equations is solved by the finite-differences numerical method. The grid region in a spherical geomagnetic coordinate system is char-

acterized by variable step along r-coordinate, 10°—along θ and 15° along λ-coordinate. A number of nodes along r, θ and λ is 30, 18 and 24, respectively. Neutral velocity equations were integrated along vertical coordinate by inexplicit numerical method. Those terms of the equations, which contained derivations on θ and λ were derived at, using previously calculated values. Neutral continuity equations and equations of heat budget were integrated by summary approximation method (MARCHUK. 1974).

The grid region in the dipole coordinate system is characterized by variable step along the flux tube of geomagnetic field which does not equal the r-coordinate step in the spherical coordinate system, and by step 8°—along θ and 15°—along λ. Maximum value of nodes along flux tube is 144.

Continuity equations and equations of heat balances for the atomic ions were integrated by means of the so-called flow trial run method (SAMARSKY, 1974).

The equation for the electric potential is approximately solved by a straightforward iterative technique.

2.6 Basic Algorithm

The main time-step of the computer program consists of several stages:

1. The input data, such as solar EUV radiation, auroral precipitation and the number of the boundary conditions, are calculated as the function of time.
2. The subsystems of the neutral atmospheric equations and subsystems molecular ion equations are calculated by iterative finite differences method in the geomagnetic spherical coordinate system.
3. The third algorithm step is a numerical interpolation of the calculated neutral atmospheric and molecular ion parameters to the nodes of the finite differences magnetic dipole coordinate grid.
4. In this stage the electric potential equations are calculated in the geomagnetic coordinate system. Both ends of all flux tubes are in the nodes of this finite differences coordinate grid.
5. The subsystem of the atomic magnetized ion continuity, momentum and energy equations is calculated by iterative finite differences method in the magnetic dipole coordinate system.
6. The numerical interpolation of the calculated ionosphere plasmasphere parameters to the geomagnetic spherical coordinate system is executed.
7. The subsystems of the neutral atmospheric equations and subsystems of the molecular ion equations are calculated with allowance for the new upper ionospheric parameters.
8. The iterative numbers of this process are determined by the task of the study. After finishing the iterative process, the next time-step of the computer algorithm is executed.

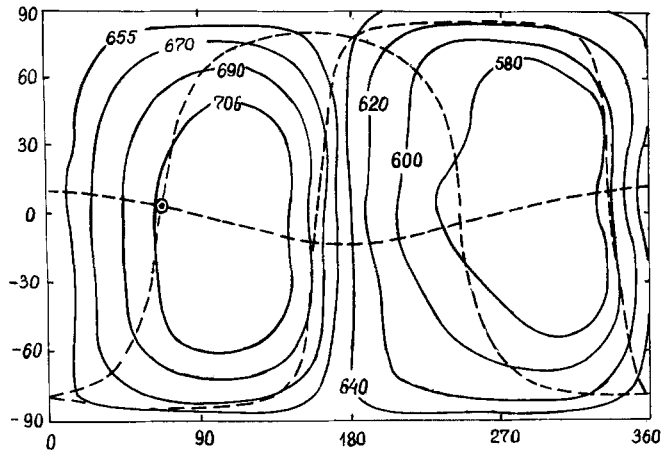

Figure 1
Contours of temperature (K) of neutral gas at 400 km in geomagnetic dipole coordinate system.

3. *Results*

In this section the results of calculations of the thermosphere-ionosphere-protonosphere system parameters are presented in the magnetic dipole latitude-longitude frame for 1200 UT. Dashed lines show the locations of the noon, midnight, sunrise and sunset geographic meridians and geographic equator in all figures. The location of the subsolar point is shown by a circle with an inner point.

Neutral Atmosphere

Figure 1 shows contours of the neutral gas temperature at 400 km. The maximum temperature is shifted in time about three hours, relative to the local noon; the ratio of the maximum temperature to the minimum temperature equals 1.3; absolute amplitude values are $T_{max.} = 720°K$, $T_{min.} = 570°K$. Figure 2 shows the plot giving the direction and magnitude of the calculated horizontal wind circulation at the altitude 400 km, and contours of vertical component of the mean-mass gas velocity are shown in Figure 3. From these figures follows, that the direction of the thermosphere gas motion is set by solar heat input, which generates wind gas flow from the dayside to the nightside.

On the dayside, neutral gas stream flows upwards, and on the night-side downwards. Maximum value of the horizontal wind velocity is about 120 m/s, and maximum value of the vertical wind velocity is approximately 2 m/s.

Figures 4–6 show contours of the decimal logarithm of the N_2, O_2 and O concentrations at 400 km. Maximum N_2 concentration is $1.1 \cdot 10^7$ cm^{-3}, minimum $\sim 4.8 \cdot 10^5$ cm^{-3}. Maximum O_2 concentration is $4.0 \cdot 10^5$ cm^{-3} and minimum $6.45 \cdot 10^3$

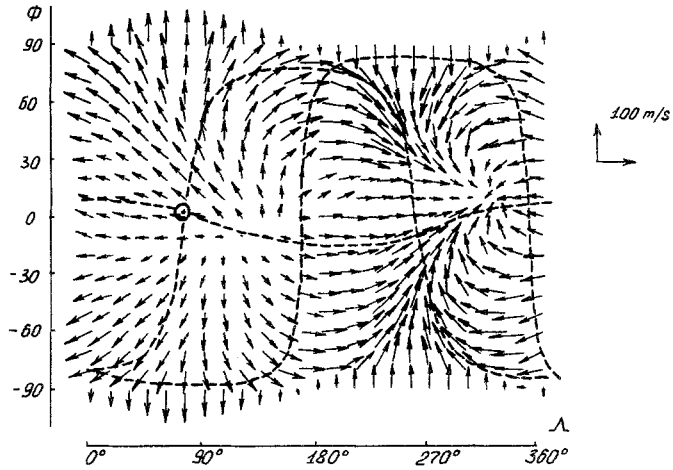

Figure 2
Calculated global distribution of horizontal neutral winds at 400 km in geomagnetic dipole coordinate system. The vectors indicate the wind direction and their length corresponds to the wind magnitude.

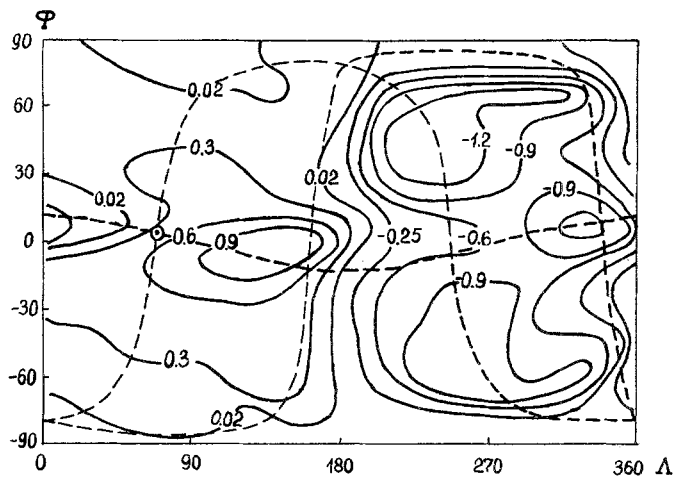

Figure 3
Contours of the vertical neutral wind (ms^{-1}) at 400 km displayed in geomagnetic dipole coordinate system.

cm^{-3}. The diurnal variation of the atomic oxygen concentration is not as large as the diurnal variations of the molecular components at 400 km. Maximal O concentration is $7.8 \cdot 10^7$ cm^{-3}, minimum concentration is $4.2 \cdot 10^7$ cm^{-3}. The diurnal harmonic predominates in the thermosphere variations at 400 km altitude for all thermospheric parameters.

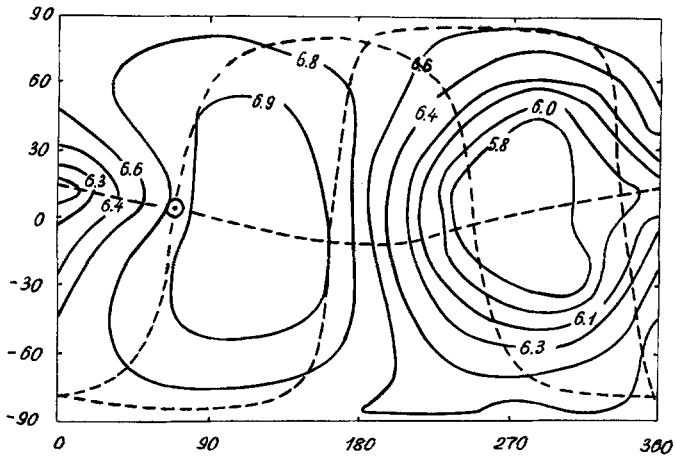

Figure 4
Contours of the $\log_{10}$ ($n(N_2)$, cm^{-3}) at 400 km in geomagnetic dipole coordinate system.

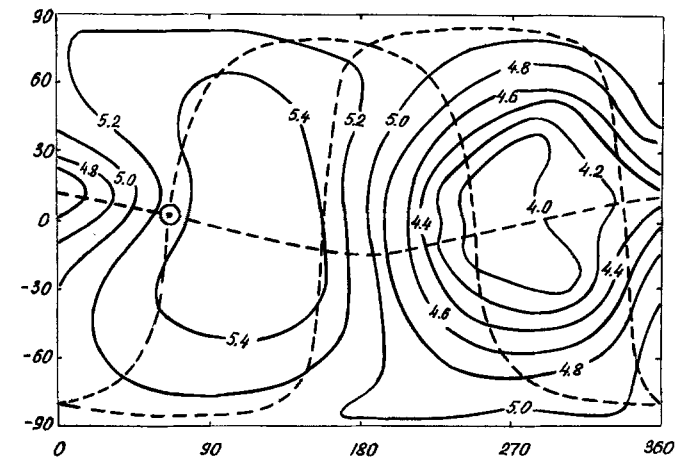

Figure 5
Contours of the $\log_{10}(n(O_2)$, $cm^{-3})$ at 400 km in geomagnetic dipole coordinate system.

Figures 7–11 show the calculated distributions of the thermospheric parameters at 120 km altitude. These distributions have essential dependence on the lower boundary conditions. Figure 7 shows contours of the neutral gas temperature on the dayside ($\sim$243°K) and two local minimum temperatures ($\sim$230°K) on the nightside in the middle latitudes. Figure 8 shows the distribution of the horizontal neutral wind velocity at 120 km altitude. The value of the vertical neutral gas velocity is $\sim$0.1 m/c and the maximum values of the horizontal wind are about 20 m/s in this altitude. Figure 9 shows contours of the decimal logarithm N_2 concentration. The

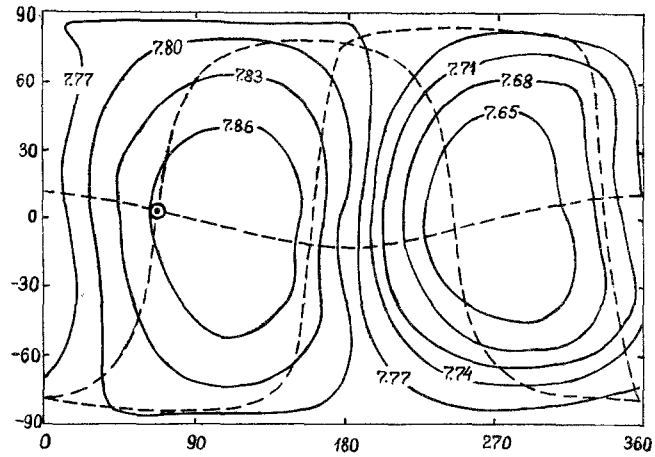

Figure 6
Contours of the $\log_{10}$ (n(O), cm^{-3}) at 400 km in geomagnetic dipole coordinate system.

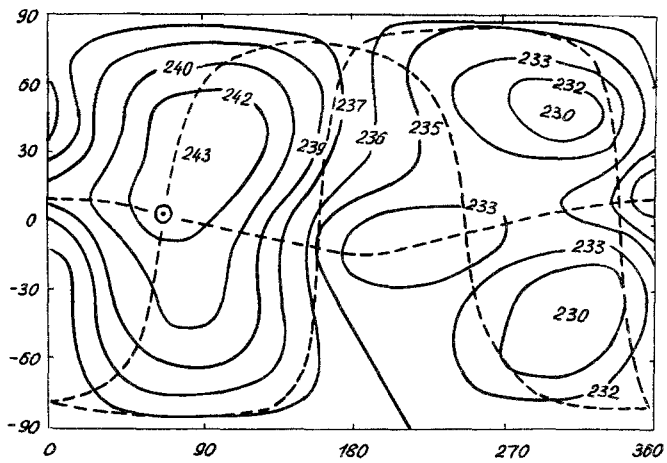

Figure 7
Contours of temperature (K) of neutral gas at 120 km in geomagnetic dipole coordinate system.

variation of this component is small at 120 km altitude (maximum N_2 concentration is $3.6 \cdot 10^{11}$ cm^{-3}, minimum $3.4 \cdot 10^{11}$ cm^{-3}). The contours of the decimal logarithm O_2 concentration are shown in Figure 10. The maximum $4.0 \cdot 10^{10}$ cm^{-3} is observed at evening local time in the middle latitudes of the southern hemisphere. The minimum O_2 concentration ($2.1 \cdot 10^{10}$ cm^{-3}) is observed at evening local time in the middle of the southern hemisphere. Figure 11 shows contours of the decimal logarithm O concentration. Maximum concentration ($1{,}4 \cdot 10^{11}$ cm^{-3}) is located in the near equatorial region at sunset local time in the northern hemisphere, and in

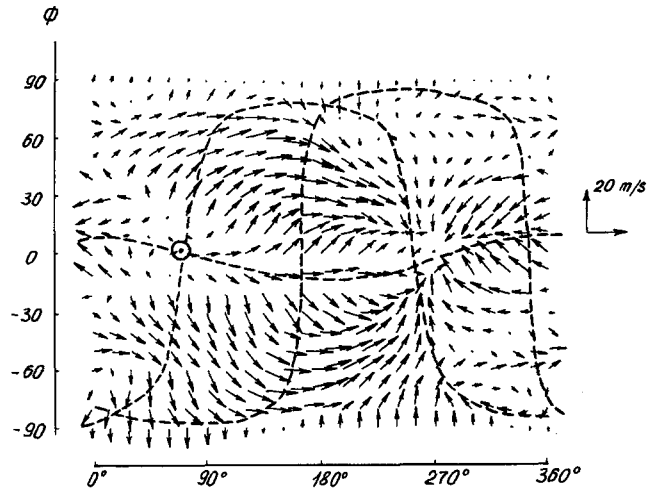

Figure 8
Calculated global distribution of horizontal neutral winds at 120 km in geomagnetic dipole coordinate system. The vectors indicate the wind direction and their length corresponds to the wind magnitude (ms^{-1}).

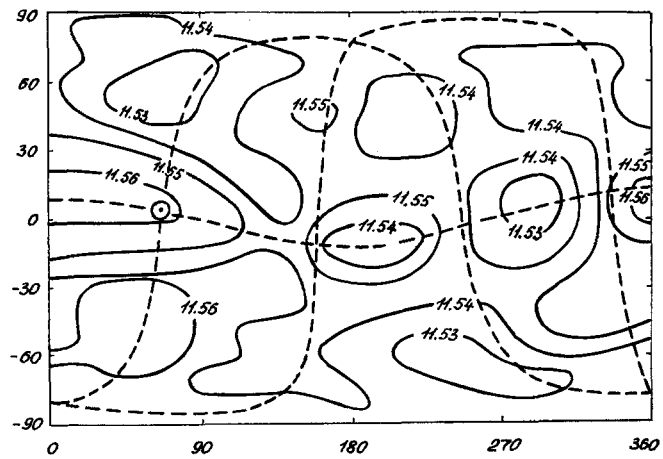

Figure 9
Contours of the $\log_{10}$ ($n(N_2)$, cm^{-3}) at 120 km in geomagnetic dipole coordinate system.

the near equatorial region of the post-midnight sector in the southern hemisphere. Minimum O concentration is in the polar regions of both hemispheres. It should be noted that variations of the neutral atmosphere parameters have both diurnal harmonic and harmonics of higher orders. Moreover, at 120 km altitude, there is no similarity between neutral concentration contours and neutral temperature contours, which have been presented at 400 km altitude.

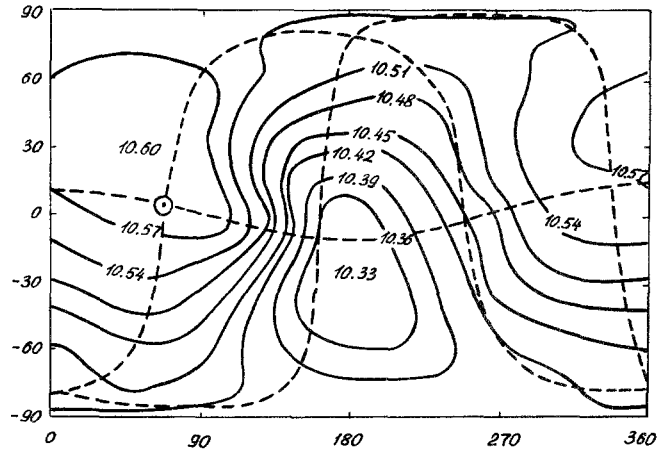

Figure 10
Contours of the $\log_{10}(n(O_2), cm^{-3})$ at 120 km in geomagnetic dipole coordinate system.

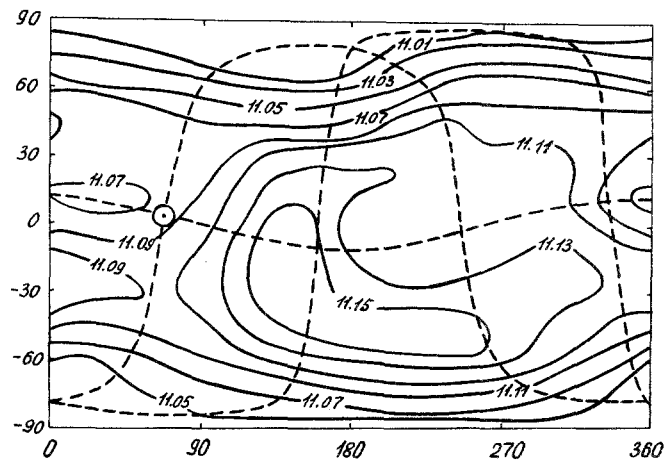

Figure 11
Contours of the $\log_{10}(n(O), cm^{-3})$ at 120 km in geomagnetic dipole coordinate system.

Lower Ionosphere

Figure 12 presents contours of the decimal logarithm XY^+ ion concentration at 120 km altitude. The XY^+ distribution is set by photochemical processes only. The highest densities are in the subsolar point and reach $1.2 \cdot 10^5$ cm^{-3}, while the lowest densities are before sunrise point and drop as low at $1.6 \cdot 10^3$ cm^{-3}. At high-latitudes ($\pm$ 70°) on the nightside the most distinct feature is the increase of the XY^+ densities reaching $8.0 \cdot 10^4$ cm^{-3}.

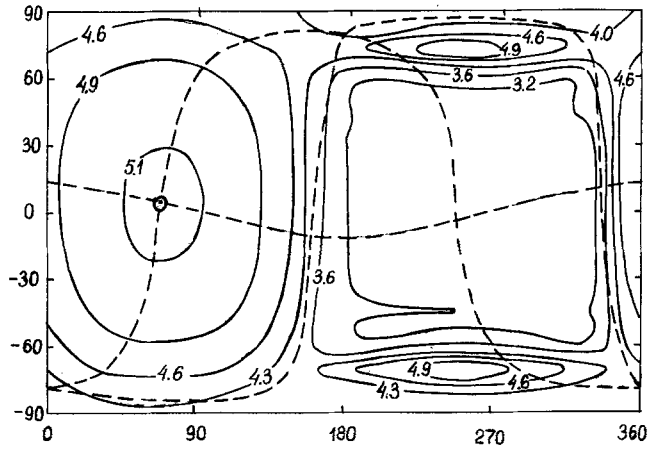

Figure 12
Contours of the $\log_{10}(n(XY^+), cm^{-3})$ at 120 km in geomagnetic dipole coordinate system.

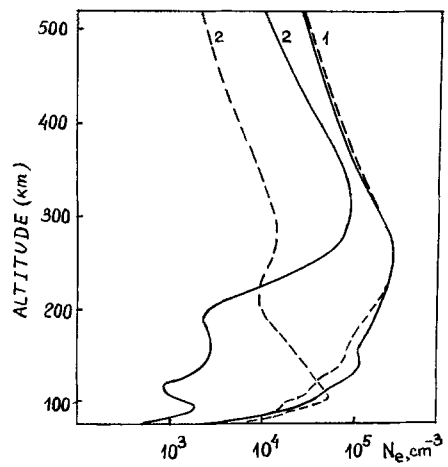

Figure 13
Altitude profiles of electron density: 1—at 90° magnetic dipole longitude, corresponding to local day-time, and 2—at 270° magnetic dipole longitude, corresponding to local night-time. Solid lines correspond to 40° magnetic dipole latitude, dashed lines—70° magnetic dipole latitude.

It is also illustrated in Figure 13, where altitude profiles of electron density are shown for day and night time on the mid-latitude and high-latitude. The increased XY^+ concentration on the high-latitude is caused by the ion production, resulting from auroral electron precipitation from the magnetosphere. The characteristic energy of the electron precipitation spectrum is 5 keV. A small asymmetry exists

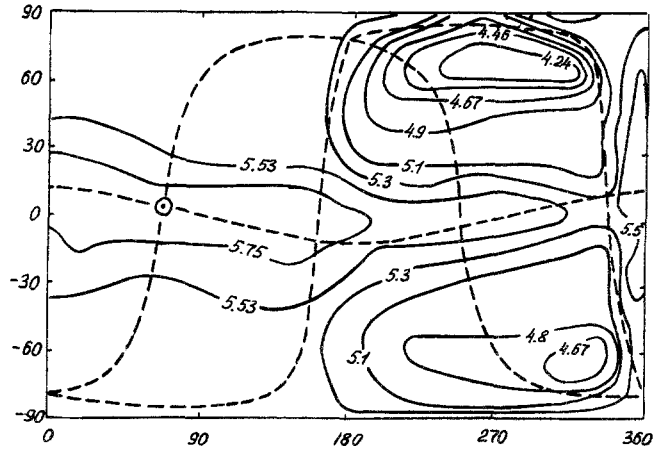

Figure 14
Contours of the $\log_{10}(N_mF2, \text{cm}^{-3})$ in geomagnetic dipole coordinate system.

between the northern and southern night hemispheres due to the offset between geomagnetic and geographic poles considered in our model.

F2-Region of Ionosphere

Figure 14 presents contours of the decimal logarithm of the electron density in the F2-region maximum, $\log_{10}(N_mF2, \text{cm}^{-3})$. The contour picture is more symmetrical regarding geomagnetic coordinates than about geographic ones, since the plasma in F2-region of the ionosphere is distributed along geomagnetic field lines. The asymmetry between hemispheres for regarded conditions is connected with the asymmetry of neutral atmosphere parameters. The maximum values of N_mF2 fall at latitudes on the post-noon hours. The absolute maximum of N_mF2 ($9.0 \cdot 10^5$ cm^{-3}) is on the geomagnetic equator. The minimum values of N_mF2 fall at night hours, decreasing to $\sim 10^4$ cm^{-3} on geomagnetic latitudes $\pm 70°$, forming troughs without sharp walls.

Figure 15 shows contours of the height of maximum ionosphere F2-region, h_mF2. There is clearly seen the control of h_mF2 by the thermosphere wind circulation. At day time, when wind direction is poleward, there is $F2$-region lowering and h_mF2 is reduced to ~ 240 km at middle latitudes. At night, when the equatorward wind is predominating, the plasma rises upward along geomagnetic field lines, and h_mF2 increases to ~ 320 km at middle latitudes. The maximum value of h_mF2 falls on near-equator region and equals ~ 350 km.

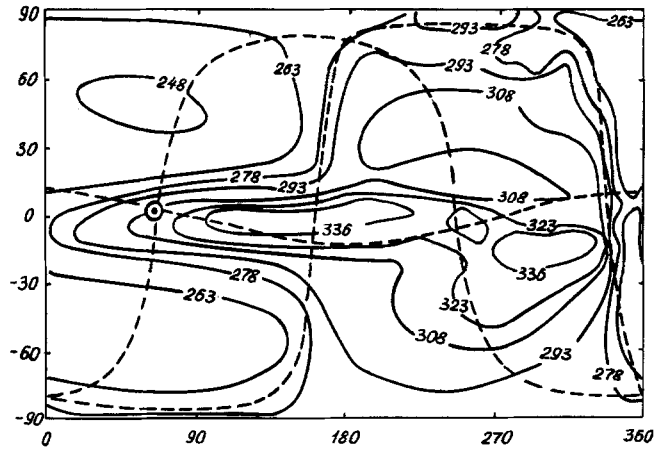

Figure 15
Contours h_mF2 (km) in geomagnetic dipole co-ordinate system.

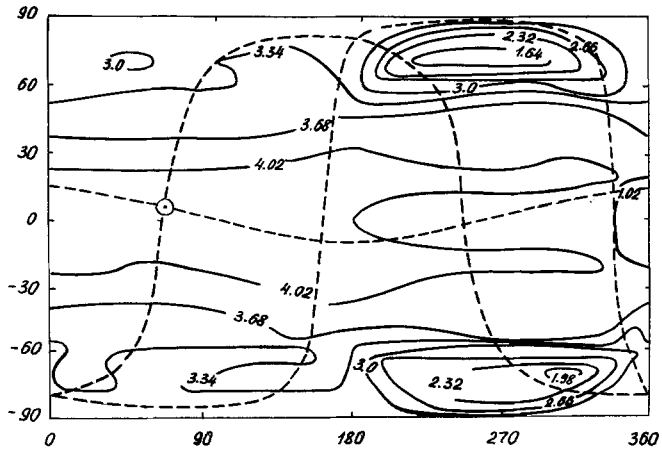

Figure 16
Contours of the $\log_{10}$ ($n(H^+)$, cm^{-3}) at 1000 km in geomagnetic dipole coordinate system.

Protonosphere

Figure 16 presents contours of the decimal logarithm of H^+ ion concentration, $\log_{10}(n(H^+), cm^{-3})$, at 1000 km altitude. The maximum values $n(H^+) \sim 10^4$ cm^{-3} fall on the low-latitude ionosphere. The H^+ ion concentration decreases with the elevation of latitude. This is explained by the growth of the flux tube volume with geomagnetic latitude as L^4 (L-parameter of McIlwain) and connected with its different state of fullness of the flux tubes. There are two 'tongues' of increased H^+ concentration on latitude $\pm 20°$, extending from dayside to nightside. The nocturnal minimum of H^+ concentration between these tongues is explained by the deficiency

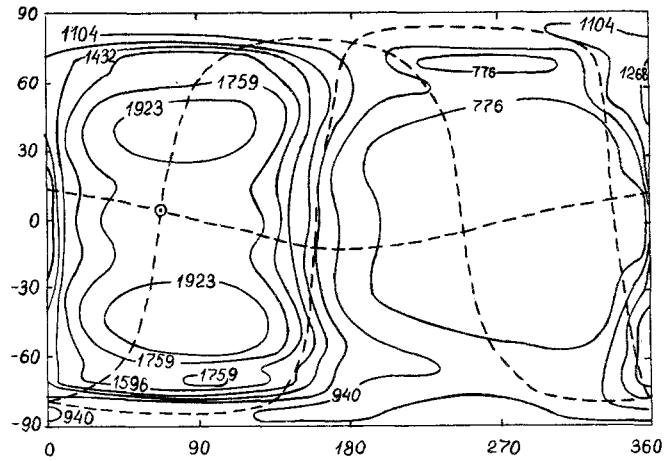

Figure 17
Contours of ion temperature (K) at 1000 km in geomagnetic dipole coordinate system.

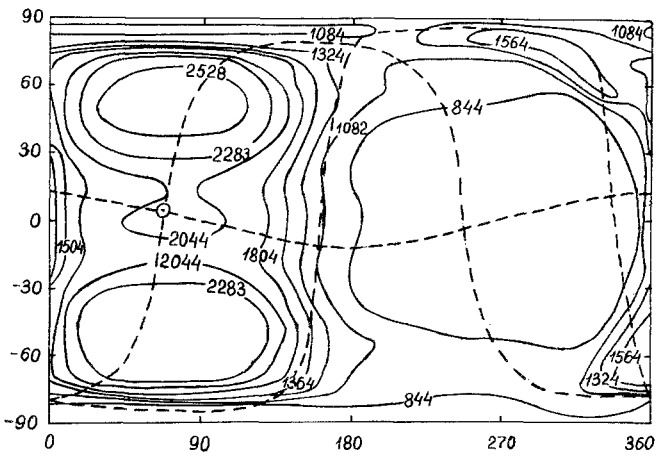

Figure 18
Contours of electron temperature (K) at 1000 km in geomagnetic dipole coordinate system.

of the plasma fluxes from a protonospheric reservoir. The distinction of the trough depths at high latitudes of the north and south hemispheres is a consequence of the asymmetry of neutral atmosphere parameters.

Figures 17–18 show contours of atomic ion and electron temperatures at 1000 km altitude respectively. The maximum values of T_e and T_i are $\sim$2800°K and 2100°K respectively, and they fall in the daytime at mid-latitudes. There is also a local maximum over the equator. At night charged particles temperatures decrease to the values close to neutral gas temperature, reaching its minimum values about

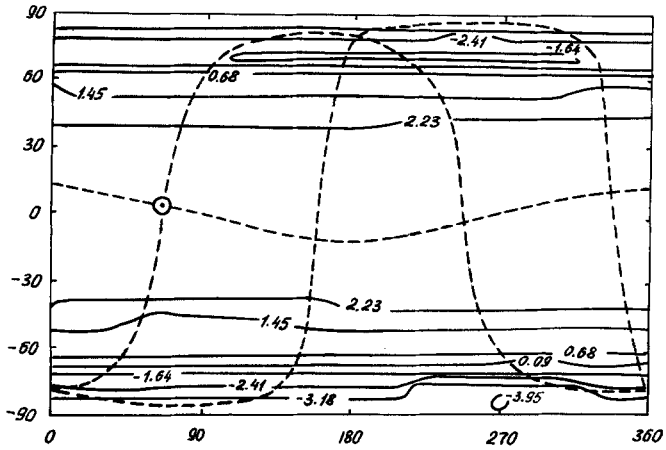

Figure 19
Contours of the $\log_{10}(n(H^+), cm^{-3})$ at 10000 km in geomagnetic dipole coordinate system.

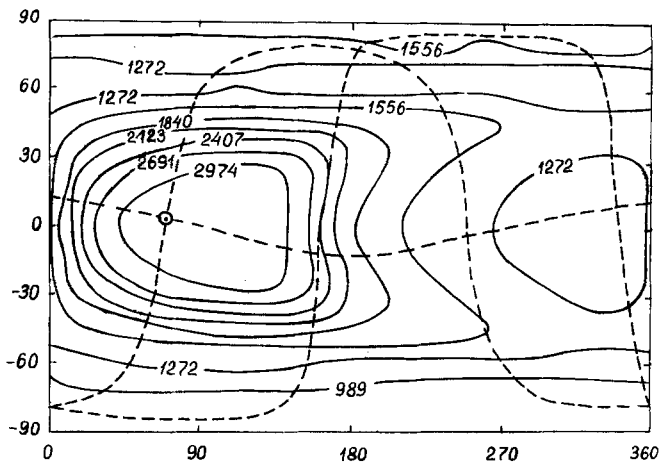

Figure 20
Contours of the ion temperature (K) at 10000 km in geomagnetic dipole coordinate system.

600°K. Figures 19–21 present contours $\log_{10}(n(H^+), cm^{-3})$, T_i and T_e at 10000 km altitude. The contours of hydrogen ion concentration are nearly parallel to geomagnetic latitude parallels, which points to the small longitude variation of H^+ concentration at this altitude. The densities of hydrogen ions decrease from 10^3 cm^{-3} at the equator to 10^{-4} cm^{-3} with the distance. The distributions of T_i and T_e at 10000 km altitude differ from those at 1000 km altitude. The temperature distributions at 1000 km have three maxima on the dayside—two absolute ones at mid-latitudes in north and south hemisphere, and one local at the equator, but at 10000 km altitude one maximum is formed at the equator with $T_i \sim 3300$°K and $T_e \sim 3700$°K.

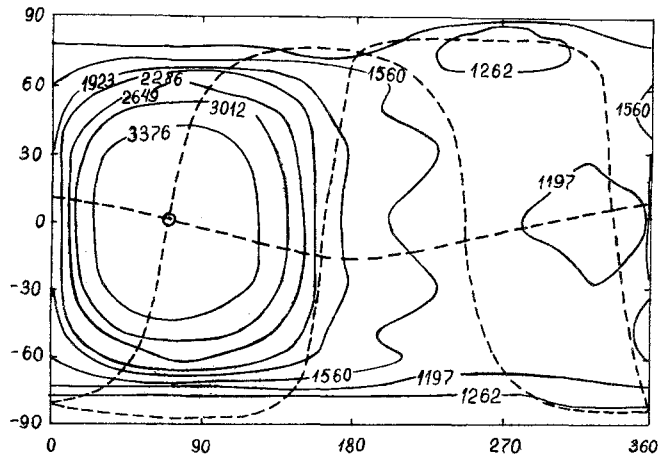

Figure 21
Contours of the electron temperature (K) at 10000 km in geomagnetic dipole coordinate system.

Electric Field Potential

Figure 22 presents calculated contours of integrated conductivities $\Sigma_{\theta\theta}$, $\Sigma_{\lambda\lambda}$ and $\Sigma_{\lambda\theta}$ which have local maximum due to electron precipitation from magnetosphere at geomagnetic latitudes $\pm 70°$ of nightside. Maximum conductivities equal approximately to corresponding conductivities at the same latitudes on the dayside. The strongest latitudinal variations take place for $\Sigma_{\theta\theta}$, which change more than three orders of value in latitudinal interval $\pm 10°$. Maximum value of $\Sigma_{\theta\theta}$ is reached at the equator on geomagnetic longitude 75° for 1200 UT and is $5.3 \cdot 10^5$ mhos. Maximum value of $\Sigma_{\lambda\lambda}$ ($1.1 \cdot 10^2$ mhos) is at the equator on the longitude 90°. Maximum values $|\Sigma_{\lambda\theta}|$ are at the latitude $\pm 5°$ on the longitude 75° for considered UT moment and equal $3.7 \cdot 10^1$ mhos.

Figure 23 presents contours of electric field potential caused by magnetospheric sources and by dynamo-effect of thermosphere circulation winds, at 175 km altitude. The potential was calculated allowing for the first and second zones of the field aligned currents located at latitudes $\pm 75°$ and $\pm 65°$, respectively. The amplitudes of accepted currents $2 \cdot 10^{-8}$ A/m^2 and $5 \cdot 10^{-9}$ A/m^2 respectively, were taken so that the calculated potential distribution of the electric field of the magnetospheric origin should correspond to quiet geomagnetic conditions. Comparing the obtained results with the model of VOLLAND (1975) shows a good agreement. The dynamo action of the thermosphere winds was taken into account in our calculations. The wind system was chosen at 175 km altitude and presumed to be uniform in the altitude region 80–

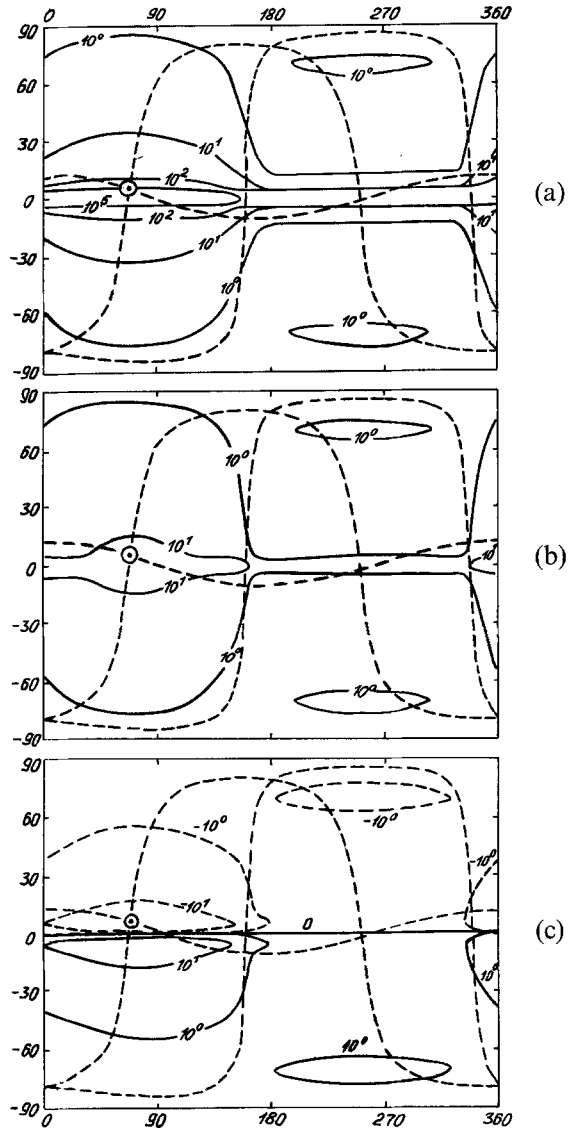

Figure 22
Contours of the integral electric conductivity (mhos): (a) $\Sigma_{\theta\theta}$, (b) $\Sigma_{\lambda\lambda}$ and (c) $\Sigma_{\lambda\theta}$ in geomagnetic dipole coordinate system.

175 km. Without considering the dynamo effect the existence region of the electric field is limited by the high latitudes. The dynamo action results in appearing of the electric field on lower latitudes in the night-time. The transformations of the electric field on the dayside are negligible and consist of the distortion of the potential contours.

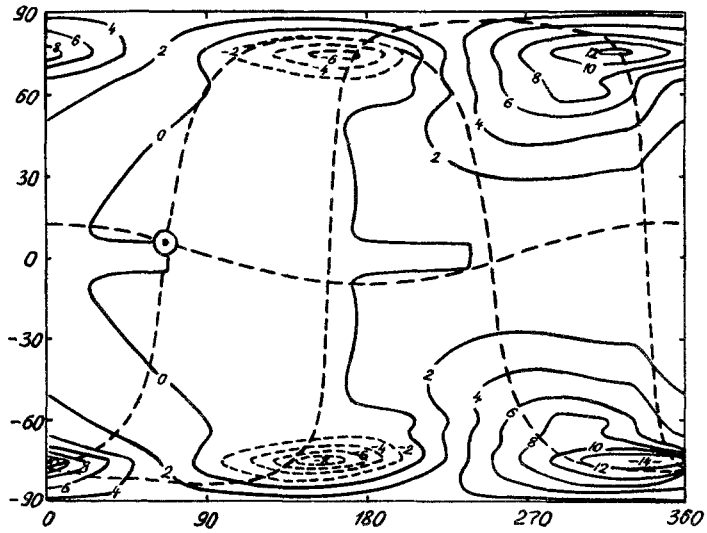

Figure 23
Contours of potential of dynamo and magnetospheric origin electric field (kV) in geomagnetic dipole coordinate system.

4. *Discussion of Results*

As we stated earlier, the calculated results in this paper are of preliminary character. We did not take into account a number of processes which could greatly influence the distribution of the calculated parameters. Moreover, the solution of the equations was being integrated only during three days, while substantially more time is needed to obtain a stationary solution of the parameters of the neutral atmosphere. The most important nonconsidered processes in the neutral atmosphere are Joule heating and tidal motions in the lower thermosphere, excited below the lower boundary of our model. The absence of Joule heating can partly account for low temperatures of the neutral atmosphere. The other possible causes are presently being analysed. The distributions of temperature and the concentrations of gases in the lower thermosphere (80–140 km) have strong dependence on the flow of particles, impulse and energy from lower layers of the atmosphere, which have been obtained by choosing lower boundary conditions. In our calculations of the lower boundary we did not consider the disturbances of the components of mean-mass velocity of the neutral gas, caused by tides coming from adjacent regions. The phase characteristics of temperature and concentrations of gases on the lower boundary were determined by the phase characteristics of the model MSIS, with corresponding parameters at the height of 120 km, which is an arbitrary assumption. The problem of the lower boundary conditions requires special research.

When calculating heat balance of the neutral atmosphere, we did not consider the heat of the lower thermosphere because of viscosity dissipation of turbulent motions. As a detailed analysis of these processes showed (GORDIETS *et al.*, 1978), the turbulent heating equals turbulent cooling. This allows no consideration of the contribution of turbulent processes in heat balance of the lower thermosphere. Moreover, we did not allow for infrared cooling from radiation particles NO ($\lambda = 5.3$ mkm). In the paper by CALEDONIA *et al.* (1982), this process is shown to be essential at large values of the temperature of neutral gas. In quiet gelio-geophysical conditions, which have been considered here, the role played by this process is small. Within the presented thermosphere model the influence study of turbulence diffusion coefficient on the gases composition of thermosphere was made. For the parameters K_m and h_m in (21–22), the magnitude and height of coefficient maximum have been varied. This led to the change of the vertical profile of the turbulence diffusion coefficient.

Figure 24a shows relative changes of the concentrations of atomic and molecular oxygen, with K_m changing and h_m having constant value. Figure 24b shows relative changes of O and O_2 when K_m has constant value, but h_m is changing. From these figures it follows, that the increase of turbulence leads to the increase of $n(O_2)$ and the decrease of $n(O)$ at heights $h = 105$ km. The concentration of molecular nitric practically does not change. All changes of the thermosphere composition, caused by the change of eddy diffusion coefficient, become localized in the region below 140 km. In our calculations the region of diffusion equilibrium of gases is above 140 km. One can draw the conclusion that the choice of K_T is seemingly unimportant for gases composition in the upper thermosphere, and is essential only for lower thermosphere, where diffusion equilibrium is absent.

In our present calculation, we are limited by the summary molecular ions compositions which can be avoided by calculations of small neutral components such as NO, $N(^4S)$, $N(^2D)$. The transport effects of the molecular ions ignored in the present model are not important in the preliminary stage because of the absence of strong electric field, as well as the absence of disturbance neutral circulation winds.

The most essential from non-accounted factors at calculations of concentrations, temperatures and velocities of charged and neutral particles is an electric field which determines the development of equatorial anomaly, troughs in F2-region and protonosphere, plasmapause, influences on the ion temperature in high-latitude ionosphere, determines Joule heating of thermosphere and changes the circulation and neutral composition.

In external ionosphere and protonosphere of high-latitudes it is necessary to consider the nonlinear term of acceleration in the equations of the motion of ions O^+, and particularly H^+ for a correct description of nonstationary processes of filling and depletion of closed plasma tubes and of a polar wind on the open field lines.

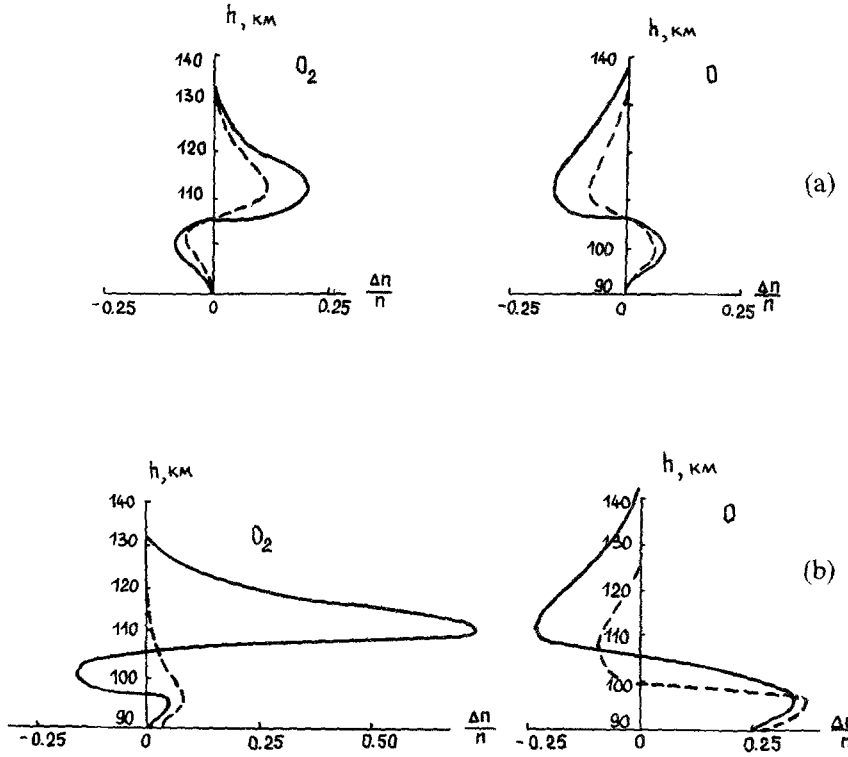

Figure 24

Variation of O and O_2 concentrations for different models of eddy diffusion coefficient: (a) ratio of O and O_2 concentrations calculated with maximum value of eddy diffusion coefficient $K_m = 1.5 \cdot 10^7$ cm^2 s^{-1} (solid lines) and with $K_m = 10^7$ cm^2 s^{-1} (dashed lines) to O and O_2 concentration calculated with $K_m = 5 \cdot 10^6$ cm^2 s^{-1}. Height of the maximum value of eddy diffusion coefficient (h_m) is 110 km; (b) ratio of O and O_2 concentrations calculated for different values h_m to O and O_2 concentrations calculated with $h_m =$ 90 km and $K_m = 1.5 \cdot 10^7$ cm^2 s^{-1} (solid lines: $h_m = 110$ km, dashed lines: $h_m = 100$ km).

It is also necessary to take into account the plasma heating by magnetospheric ring current, and to calculate the vibrational temperature N_2 molecules and dependence of the loss rate of O^+ ions from it. This will allow refinements of the description of O^+ ions loss, particularly in disturbed periods.

Presented calculation results of electric field potential were received without allowing for the electric fields influence on ionosphere and thermosphere. Under selfconsistent calculation of all parameters there will be changes both in conductivities and thermospheric circulation, which in its turn will be reflected in potential distribution. The essential influence on electric field potential distribution can effect a correct choice of low boundary conditions for thermosphere, which will change the

vertical structure of thermospheric circulation and the dynamo field, respectively. The consideration of hot particles in magnetosphere and selfconsistent calculations of their distribution will allow the calculation of field aligned currents of the second zone and particle precipitation selfconsistently. Using dependence of field aligned currents of the first and third zones with parameters of IMF, solar wind and geomagnetic activity indices, will permit calculation of disturbed situations by means of those currents. We hope to consider all above-mentioned factors in future.

5. *Conclusion*

In this paper we have formulated the task and have given preliminary results of the calculations of the parameters of thermosphere, ionosphere, protonosphere as an integrated system. The constructed model describes global distribution of the parameters of many-component near-earth plasma at the heights from 80 km to 15 earth's radii and its changes with time; it also takes account of offset of geographic and geomagnetic poles of the earth. The model consists of three main blocks: thermosphere, ionosphere-protonosphere blocks and the block of the calculation of electric fields. The thermosphere block considers the global nonstationary distribution of the neutral gas temperatures, concentration of the basic neutral O_2, N_2, O and three-dimensional circulation of the neutral gas in the region of heights 80–520 km. At higher altitudes for all neutral components diffusion balance is assumed at temperatures not varying with altitude. For calculation of the distribution of the neutral hydrogen concentration, boundary condition is used at the altitude 500 km from the model by JACCHIA (1977). In the presented thermosphere model the following processes are taken into account: turbulent and molecular diffusion for all components of neutral gas; three-dimensional circulation of neutral gas; chemical processes; the heating of the atmosphere by solar ultraviolet radiation and fluxes of precipitating electrons; and the processes of heat conductivity and cooling of the neutral gas due to infrared radiation.

The ionosphere block of the model calculates the global nonstationary distribution of the molecule and atom ions concentration; ion and electron temperatures.

Calculations of the molecule ions concentration are made in photochemical approximation with provision for the processes of ionization by direct and scattered UV radiation of Sun and precipitating electrons. The preliminary calculations of the atom ions O^+ and H^+ concentration and the heat balance of ions and electrons are performed with consideration of the processes of diffusion thermosphere winds, chemical reactions, ionization by the Sun's UV radiation and the fluxes of precipitating particles, as well as processes of heat and mass exchanges between ionosphere and plasmophere.

The calculations of the global two-dimensional distribution of an electric

potential are made by calculating in our model thermosphere-ionosphere parameters and the given distribution of field aligned currents in high latitude ionosphere.

The input parameters of the model are fluxes of the solar ionizing and dissociation radiation, spectral density of the energy of precipitating electrons and their spatial distributions, the values and the spatial distribution of field aligned currents, the model of magnetic field.

With determined initial input parameters and boundary conditions the whole system of model equations is solved by different iteration methods in two coordinate systems. The equations describing the behavior of thermosphere parameters, molecule ions and electric potential are solved in a spheric geomagnetic system of coordinates. The equations of continuity and motion of atom ions and the equations of heat balance of magnetized plasma are integrated in a dipole system of coordinates along force lines of the geomagnetic field.

The exchange of information between the blocks of the model proceeds by means of interpolation of necessary parameters from the knots of difference network of one system of coordinates into the other and *vice versa.*

For preliminary calculations, we have taken conditions of spring equinox, low sun and geomagnetic activities and have presented results for 1200 UT, in the form of global distributions of the calculated parameters.

Studying the possibilities of the model we first confined ourselves to the consideration of the role of heat source and ionization in the global distribution of the sought parameters, without considering electromagnetic drifts of heat plasma. The results of the calculations showed correct functioning of the bases algorithm of the model, because they do not contradict the existing idea of global distribution of the considered parameters, resulting from the action of physical mechanisms accounted in the model. At the next stage of our research we hope to study the influence of nonstationary electromagnetic drift of thermal plasma on the global distribution of the parameters of the thermosphere-ionosphere-protonosphere system. In the future we shall transfer to the study of global dynamics of the effects of magnetic storms and substorms in near-earth plasma.

References

ALCAYDE, D. (1981), *An analytical static model of temperature and composition from 20 to 2000 km altitude.* Ann. Geophys. *37*, 515–528.

ANDERSON, D. N. (1973), *A theoretical study of the ionospheric F-region equatorial anomaly—1. Theory.* Planet. Space Sci. *21*, 409–419.

ANDERSON, D. N. (1981), *Modelling the ambient, low latitude F-region ionosphere—A review.* J. Atmos. Terr. Phys. *43*, 753–762.

BAILEY, G. J. (1978), *Interhemispheric flow of thermal plasma in a closed magnetic flux tube at mid-latitudes under sunspot minimum conditions.* Planet. Space Sci. *26*, 753–765.

CALEDONIA, G. E. and KENNEALY, J. P. (1982), *NO infrared radiation in the upper atmosphere.* Planet. Space Sci. *30*, 1043–1055.

DEMINOV, M. G. and HEGAI, V. V. (1981), *Analytical approximation of the ionization production rate by auroral electrons* (in Russian). Geomag. i Aeronomiya *20*, 145–147.

DICKINSON, R. E., RIDLEY, E. C. and ROBLE, R. C. (1981), *Three-dimensional general circulation model of the thermosphere.* J. Geophys. Res. *86*, 1499–1512.

DICKINSON, R. E., RIDLEY, E. C. and ROBLE, R. C. (1984), *Thermospheric general circulation with coupled dynamics and composition.* J. Atmos. Sci. *41*, 205–219.

FEJER, B. G., FARLEY, D. T., WOODMAN, R. F. and CALDERON, C. (1979), *Dependence of equatorial F-region vertical drifts on season and solar cycle.* J. Geophys. Res. *84*, 5792–5796.

FULLER-ROWELL, T. J. and REES, D. (1980), *A three-dimensional time-dependent global model of the thermosphere.* J. Atmos. Sci. *37*, 2545–2567.

FULLER-ROWELL, T. J. and REES D. (1983), *Derivation of conservation equation for two-constituent gas within a three-dimensional time-dependent model of the thermosphere.* Planet. Space Sci. *31*, 1209–1222.

GIZLER, V. A., SEMENOV, V. S. and TROSHICHEV, O. A. (1979), *Electric fields and currents in the ionosphere generated by field aligned currents observed by Triad.* Planet. Space Sci. *27*, 223–231.

GLUSHAKOV, M. L. (1979), *About large-scale electric field in the dynamo-region of the ionosphere* (in Russian). Geomag. i Aeronomiya *19*, 45–52.

GORDIETS, B. F., MARKOV, M. N. and SHELEPIN, L. A. (1978), *IR-radiation of the upper atmosphere.* Planet. Space Sci. *26*, 933–947.

GORDIETS, B. F., KULIKOV, YU. N., MARKOV, M. N. and MAROV, M. YA. (1982), *Numerical modeling of the thermosphere heat budget.* J. Geophys. Res. *87*, 4504–4514.

HARDY, D. A. and GUSSENHOVEN, M. S. (1985), *A statistical model of auroral electron precipitation.* J. Geophys. Res. *90*, 4229–4248.

HAREL, M., WOLF, R. A., REIFF, P. H., SPIRO, R. W., BURKE, M. J., RICH, F. J. and SMIDDY, M. (1981), *Quantitative simulation of a magnetospheric substorm. 1. Model logic and overview.* J. Geophys. Res. *86*, 2217–2241.

HEDIN, A. E., REBER, C. A., NEWTON, N. W., SPENCER, N. W., BRINTON, H. C., MAYR, H. G. and POTTER, W. E. (1977), *A global thermospheric model based on mass-spectrometer and incoherent scatter data, MSIS2, composition.* J. Geophys. Res. *82*, 2148–2156.

IIJIMA, T., POTEMRA, T. A. (1976), *The amplitude distribution of field-aligned currents at northern high latitudes observed by Triad.* J. Geophys. Res. *81*, 2165–2174.

IVELSKAYA, M. K., IVANOV-KHOLODNY, G. S., KATYUSHINA, V. V. and KLIMOV, N. N. (1970), *Daily variations of oxygen in the region of 65–200 km* (in Russian). Geomag. i Aeronomiya *10*, 1048–1052.

JACCHIA, L. G. (1977), *Thermospheric temperature, density and composition: New models.* SAO Special Report, N 375, pp. 106.

KARPOV, I. V., SMERTIN, V. M. and BESSARAB, F. S. *Three-dimensional, time-dependent model of the thermosphere* (in Russian), In *Ionosph. Issled.* N42 (Sov. Radio, Moscow. 1987), pp. 90–94.

KLIMENKO, V. V. and NAMGALADZE, A. A. (1980), *About the role of convection in formation of trough and plasmapause* (in Russian). Geomag. i Aeronomiya *20*, 946–950.

KLIMENKO, V. V. (1983), *Role of ions motion inertia in formation of trough and plasmapause* (in Russian). Geomag. i Aeronomiya *23*, 915–918.

KNUDSEN, W. C. (1974), *Magnetospheric convection and the high-latitude F2 ionosphere.* J. Geophys. Res. *79*, 1046–1055.

KNUDSEN, W. C., BANKS, P. M., WINNIGHAM, J. D., KLUMPAR, D. M. (1977), *Numerical model of the convecting F2 ionosphere at high latitudes.* J. Geophys. Res., *82*, 4784–4792.

KOLESNIK, A. G. and GOLIKOV, I. A. (1982), *Three-dimensional model of high-latitude F-region with accounting of offset between geographic and geomagnetic co-ordinates* (in Russian). Geomag. i Aeronomiya *22*, 725–731.

KOLESNIK, A. G. and KOROLEV, S. S. (1983), *Three-dimensional model of the thermosphere* (in Russian). Geomag. i Aeronomiya *23*, 774–781.

KRINBERG, I. A. and TASHCHILIN, A. V. (1980), *The influence of the ionosphere-plasmasphere coupling upon the latitude variations of ionospheric parameters.* Ann. Geophys. *36*, task. 4, 537–548.

LAYTSKY, W. B. *Current systems of magnetosphere-ionosphere disturbances* (in Russian) (Nauka, Leningrad, 1978), pp. 200.

MARCHUK, G. I. (1974), *A numerical solution of dynamical problems of ocean and atmosphere* (in Russian) (Gidrometeoizdat, Leningrad, 1974), pp. 303.

MARUBASHI, K. (1979), *Effects of convection electric fields on the thermal plasma flow between the ionosphere and the protonosphere.* Planet. Space Sci. *27*, 603–615.

MATAFONOV, G. K. (1986), *Distribution of energy losses of photoelectrons between ionosphere and plasmasphere* (in Russian), In *Issled. Geomag. Aeronom. i Phys. Solnca*, N75, 73–78.

MOFFET, R. J., MURPHY, J. A. (1973), *Coupling between the F-region and protonosphere: numerical solution of the time-dependent equations.* Planet. Space Sci. *21*, 43–52.

MOZHAEV, A. M. and OSIPOV, N. K. (1977), *Polar ionosphere structure and magnetospheric plasma convection beyond the plasmapause* (in Russian). Geomag. i Aeronomiya *17*, 273–279.

MOZHAEV, A. M. and OSIPOV, N. K. (1981), *Analytical models of electric field and field-aligned currents* (in Russian). Geomag. i Aeronomiya *21*, 346–351.

NAMGALADZE, A. A., LATISHEV, K. S., KORENKOV, YU. N. and ZAKHAROV, L. P. (1977), *Dynamical model of the mid-latitude ionosphere for a height range from 100 to 1000 km.* Acta Geophys. Polonica *25*, 173–182.

NAMGALADZE, A. A., KLIMENKO, V. V. and SAENKO, YU. S. *Modelling of the ionospheric trough and plasmapause* (in Russian). In *Dynam. Proc. i Struk. Pol. Ionosph.* (Nauka, Apatity, 1980), pp. 3–10.

NAMGALADZE, A. A., KORENKOV, YU. N., KLIMENKO, V. V., KARPOV, I. V. and SUROTKIN, V. A. *The global prediction model of the disturbance ionosphere. Formulation of the task* (in Russian). In *Prognoz. Ionosph. i Uslov. Rasp. Radiovoln* (Nauka, Moscow, 1985), pp. 3–13.

OGAWA, T. and SHIMAZAKI, T. (1975), *Diurnal variations of odd nitrogen and ionic densities in the mesosphere and lower thermosphere: simultaneous solution of photochemical-diffusive equations.* J. Geophys. Res. *80*, 3945–3960.

POLJAKOV, V. M., POPOV, G. V., KOEN, M. A. and KHAZANOV, G. V. (1975), *A mathematical model of dynamics and energetics of the plasma component in the ionosphere and the plasmasphere* (in Russian). In *Issled. Geomag. Aeronom. i Phys. Solnca*, N33, pp. 3–16.

PUDOVKIN, M. I. and ZAKHAROV, V. E. *Dynamic processes investigation in magnetospheric plasma* (in Russian), In *Magnetosph. Issled.* (Radio i Svajz, Moscow, 1984), N2, pp. 67–85.

QUEGAN, S., BAILEY, G. J., MOFFET, R. J., HEELIS, R. A., FULLER-ROWELL, T. J., REES, D. and SPIRO, R. W. (1982). *A theoretical study of the distribution of ionization in the high-latitude ionosphere and the plasmasphere: First results on the mid-latitude trough and the light-ion trough.* J. Atmos. Terr. Phys. *44*, 619–640.

RICHMOND, A. D., BLANC, M., EMERY, B. A., WAND, R. H., FEJER, B. G., WOODMAN, R. F., GANGULY, S., AMAYENC, P., BEHNKE, R. A., CALDERON, C. and EVANS, J. V. (1980), *An empirical model of quiet-day ionospheric electric fields at middle and low latitudes.* J. Geophys. Res. *85*, 4658–4664.

SAENKO, YU. S., NATSVALYAN, N. S., TEPENITSYNA, N. YU. and YAKIMOVA, G. A. *A simple three-dimensional model of F2-layer of ionosphere* (in Russian). In *Variacii Ionosph. vo Vremya Magnetosph. Vozmush.* (Nauka, Moscow, 1980), pp. 11–16.

SAMARSKY, A. A. (1974), *Introduction to the Difference Scheme Theory* (in Russian), Nauka, Moscow), pp. 552.

SCHUNK, R. W. and WALKER, J. C. G. (1972), *Oxygen and hydrogen ion densities above Millstone Hill.* Planet Space Sci. *20*, 581–589.

SCHUNK, R. W. and WALKER, J. C. G. (1973), *Theoretical ion densities in the lower ionosphere.* Planet Space Sci. *21*, 1875–1896.

SCHUNK, R. W. and RAITT, W. J. (1980), *Atomic nitrogen and oxygen ions in the daytime high-latitude F-region.* J. Geophys. Res. *85*, 1255–1272.

SEREBRYAKOV, B. E. (1982), *Investigation of processes in the thermosphere during the magnetic disturbances* (in Russian). Geomag. i Aeronomiya *22*, 776–782.

SHIMAZAKI, T. (1971), *Effective eddy diffusion coefficient and atmospheric composition in the lower thermosphere.* J. Atmos. Terr. Phys. *33*, 1383–1401.

SOJKA, J. J., RAITT, W. J. and SCHUNK, R. W. (1981a), *A theoretical study of the high-latitude winter F-region of solar minimum for low magnetic activity.* J. Geophys. Res. *86*, 609–621.

SOJKA, J. J., RAITT, W. J. and SCHUNK, R. W. (1981b), *Theoretical predictions for ion composition in the high-latitude winter F-region for solar minimum and low magnetic activity.* J. Geophys. Res. *86*, 2206–2216.

SOJKA, J. J., RAITT, W. J. and SCHUNK, R. W. (1981c), *Plasma density features associated with strong convection in the winter high-latitude F-region.* J. Geophys. Res. *86*, 6968–6976.

SOJKA, J. J. and SCHUNK, R. W. (1985), *A theoretical study of the global F-region for June solstice, solar maximum and low magnetic activity.* J. Geophys. Res. *90*, 5285–5298.

STUBBE, P. (1970), *Simultaneous solution of the time-dependent coupled continuity equations, heat conduction equations and equations of motion for a system consisting of a neutral gas, an electron gas and a four-components ion gas.* J. Atmos. Terr. Phys. *32*, 865–903.

STUBBE, P. and WARNUM, W. S. (1972), *Electron energy transfer rates in the ionosphere.* Planet. Space Sci. *20*, 1121–1126.

SUROTKIN, V. A., KLIMENKO, V. V. and NAMGALADZE, A. A. *Numerical model of the equatorial ionosphere* (in Russian). In *Issled. Ionosph. Dynam.* (IZMIRAN, Moscow, 1979), pp. 58–68.

TAKEDA, M. (1982), *Three-dimensional ionospheric currents and field aligned currents generated by asymmetrical dynamo action in the ionosphere.* J. Atmos. Terr. Phys. *44*, 187–193.

TORR, D. G. and TORR, M. R. (1979), *Chemistry of the thermosphere and ionosphere.* J. Atmos. Terr. Phys. *41*, 797–839.

VLASOV, M. N. and DAVYDOV, V. E. (1981), *Investigation of theoretical description of distribution of the main neutral components of the upper atmosphere* (in Russian). Geomag. i Aeronomiya *21*, 683–688.

VOLLAND, H. (1975), *Models of global electric fields within the magnetosphere.* Ann. Geophys. *31*, 159–173.

VOLLAND, H. (1978), *A model of the magnetospheric electric convection field.* J. Geophys. Res. *83*, 2695–2699.

WAGNER, C. U., MOHLMAN, D., SCHAFER, K. MISHIN, V. M. and MATVEEV, M. I. (1980), *Large-scale electric fields and currents and related ferromagnetic variations in the quiet plasmasphere.* Space Sci. Rev. *26*, 392–446.

WOLF, R. A. (1970), *Effects of ionospheric conductivity on convective flow of plasma in the magnetosphere.* J. Geophys. Res. *75*, 4677–4698.

WOLF, R. A. and JAGGI, R. K. (1973), *Can the magnetospheric electric field penetrate to the low-latitude ionosphere?* Comm. Astroph. and Space Phys. *5*, 99–107.

YOUNG, E. R., TORR, D. G. RICHARDS, P. and NAGY, A. F. (1980), *A computer simulation of the mid-latitude plasmasphere and ionosphere.* Planet. Space Sci. *26*, 881–893.

(Received 3rd May, 1987, revised 2nd June, 1987, accepted 5th July, 1987)